

Vapor-phase synthesis of 3-methylindole from glycerol and aniline over zeolites-supported Cu-based catalysts

Yanxi Cui, Xiaoshuang Zhou, Qi Sun, Lei Shi*

Institute of Chemistry for Functionalized Materials, Liaoning Normal University, Dalian 116029, China



ARTICLE INFO

Article history:

Received 13 April 2013

Accepted 21 June 2013

Available online 1 July 2013

Keywords:

3-Methylindole

Zeolites-supported copper-based catalysts

NaY

Sodium oxide

Glycerol

ABSTRACT

Zeolites-supported Cu-based catalysts for the vapor-phase synthesis of 3-methylindole from glycerol and aniline were investigated. The catalysts were characterized by N₂ adsorption, XRD, NH₃-TPD and TG-DTA techniques. The results indicated that Cu/NaY catalyst exhibited higher activity and selectivity than Cu/5A, Cu/HZSM-5 or Cu/MCM-41 due to better dispersion of copper particles and larger amount of weak acid sites on the catalyst. The addition of Na₂O to Cu/NaY not only improved the selectivity of the catalyst efficiently, but also inhibited the deactivation of the catalyst. Over Cu/NaY-Na₂O, the selectivity of 3-methylindole reached 72.3% and the yield of the aim product was up to 50.4%. The characterizations revealed that Na₂O promoter could decrease the amount of middle-strong acid sites of the catalyst remarkably as well as prevent from the formation of the coke. Furthermore, a probable catalytic mechanism for the synthesis of 3-methylindole from glycerol and aniline was proposed.

© 2013 Elsevier B.V. All rights reserved.

1. Introduction

Recently, much attention has been given to the use of glycerol for glycerol is the main by-product (about 10 wt%) in biodiesel production [1–5]. Finding out new outlets to make good use of the surplus glycerol agrees with the concept of green chemistry in terms of the utilization of renewable resources and can accelerate the development of biodiesel. Up to now, many efforts have been put toward the conversion of glycerol and many value-added chemicals are obtained such as propanediols, acrolein, glyceric acid, methyl glycerate, solketal and ethylene glycol [6–11].

3-Methylindole, an important nitrogen-containing heterocyclic chemical, can be widely applied in the fields of industry, agriculture and medicine [12–14]. For example, it can be used in perfumes and in the manufacture of herbicides, fungicides, dyes, antihypertensive, anti-diuretic, muscular relaxant and anticancer medicaments [15,16]. Recently, 3-methylindole was found other interesting uses, such as, affecting the production of serotonin, hemolyzing bovine erythrocytes, activating transcription of cytochrome P450 enzymes in hepatocytes and a broad bacteriostatic effect on some gram-negative enterobacteria [17–20].

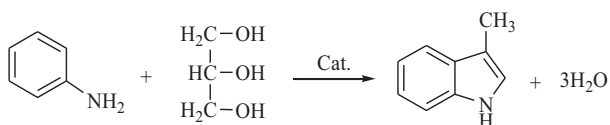
For many years, the synthesis of 3-methylindole has been an area of focus for the chemists engaged in fine chemicals synthesis and numerous methods have been developed [21,22]. Among them, liquid-phase method is often considered conventional because it

can give 3-methylindole in a good yield [23,24], however, some drawbacks exist, such as the use of complicated and expensive reagents or catalysts, a large number of toxic solvents and heavy pollution [25–27], which has limited the further development of 3-methylindole. Thus, increasing interest has been focused on the vapor-phase synthesis of 3-methylindole. Subrahmanyam and co-workers [28] carried out the reaction from indole and methanol (molar ratio of indole/methanol was 1:6) over CeHY zeolite catalyst and a 33% yield of 3-methylindole was obtained. Vaccari and co-workers [29] conducted the synthesis of 3-methylindole from 1,2-propanediol and aniline over ZrO₂/SiO₂ catalyst, but the yield of 3-methylindole was only 12%. Recently, our group developed a new approach for the vapor-phase synthesis of 3-methylindole with feeding glycerol and aniline as reactants (Scheme 1). Over Cu/SiO₂–Al₂O₃, the yield of 3-methylindole reached 40% [30]. Since glycerol, comes from biomass, is not only cheap and abundant, but also a green feedstock, this synthesis, from the economic and environmental viewpoints, can be considered a most promising route.

In the last few decades, zeolites have attracted increasing interest in the catalytic synthesis of fine chemicals because of their special features such as the acidity, the inherent capability of product selectivity, commercially available, non-corrosive and eco-friendly nature, etc [31–34]. The objective of this work is to research zeolites (NaY, 5A, HZSM-5 and MCM-41)-supported copper catalysts for the vapor phase synthesis of 3-methylindole from glycerol and aniline. Na₂O promoter was introduced into the optimal zeolite-supported copper catalyst to increase the selectivity of 3-methylindole. BET, XRD, NH₃-TPD and TG-DTA techniques were used to reveal the relationship between the structure of catalysts

* Corresponding author. Tel.: +86 411 82158329; fax: +86 411 82158309.

E-mail addresses: shilei515@dl.cn, shilei515@hotmail.com (L. Shi).



Scheme 1. Vapor-phase synthesis of 3-methylindole from glycerol and aniline.

and their catalytic performances. Moreover, a probable catalytic mechanism for the synthesis of 3-methylindole was suggested.

2. Experimental

2.1. Materials

The zeolites of NaY and 5A were obtained from Shanghai Hengye Molecular Sieve Co. Ltd. (China). HZSM-5 zeolite was obtained from Nankai Chemical Co. Ltd. (China). MCM-41 was prepared as described in Ref. [35] and the XRD pattern of MCM-41 sample is depicted in Fig. 1. A dominant (100) peak centered at about 2° was appeared, as well as the additional weak (110) and (200) peaks were also obviously observed, corresponding to a highly ordered 2D-hexagonal mesoporous silica framework.

2.2. Catalyst preparation

The zeolite (NaY, 5A, HZSM-5 or MCM-41)-supported copper catalyst was prepared by equal volume impregnation. After impregnating the zeolite support (20–40 mesh) in copper nitrate aqueous solution for 15 h at room temperature, the sample was dried at 120 °C for 4 h, then, calcined at 500 °C for 4 h to obtain the catalyst precursor. Cu/NaY-Na₂O catalyst was prepared by sequential impregnation. Na₂O was first loaded on the surface of NaY, followed by copper and the process was the same as zeolite-supported copper catalyst described above.

Prior to activity test, 3 mL catalyst precursor was in situ reduced in a gas mixture composed of N₂ (30 mL/min) and H₂ (30 mL/min) at 250 °C for 2 h, then cooled to 220 °C in 0.5 h and kept at the temperature for another 0.5 h. Copper loading was 5.4 wt%.

2.3. Catalyst characterization

BET surface areas and pore volumes of the catalysts were determined by pure nitrogen adsorption using an AUTOSORB-1MP apparatus. Before each measurement, the sample was outgassed overnight at 200 °C under 10⁻³ Torr. Calculation of pore sizes followed the method of Barret–Joyner–Halenda (BJH) according to the desorption portion of the isotherms.

X-ray diffraction (XRD) patterns were recorded by using a D8 Advance diffraction meter with Cu K α source. MCM-41 sample was scanned in the 2θ range of 0.5–10° in steps of 1°/min, while, zeolites-supported Cu-based catalysts were scanned from 30° to 80° at a rate of 0.5°/min. The voltage and current were 40 kV and 40 mA, respectively. Average copper crystallite size was calculated from peak broadening using Scherrer equation:

$$D = \frac{K\lambda}{\beta \cos \theta}$$

where K is the shape factor (0.89 for the present instrument), λ is the wavelength of X-ray, typically 1.54 Å (Cu K α), β is the line broadening at half the maximum intensity (FWHM) in radians, and θ is the Bragg angle, D is the crystallite size.

The temperature programmed desorption of ammonia (NH₃-TPD) was carried out in a quartz reactor with inside diameter of 6 mm and length of 350 mm. A 150 mg sample was pretreated at 500 °C for 1 h in a flow of ultrapure helium gas (35 mL/min) to remove water and other contaminants from the catalyst and cooled down to 100 °C, then saturated with ammonia gas at 100 °C. After the sample was purged with helium gas (35 mL/min) at 100 °C for 2 h to remove physisorbed ammonia, TPD was carried out from 100 to 700 °C with a temperature ramp of 10 °C/min.

Thermogravimetric and differential thermal analysis (TG-DTA) was carried out with a Diamond 6300 apparatus to characterize the coke on the catalyst. About 7.8 mg of the used catalyst (all the used catalysts were proceeded the same reaction time of 4 h) was placed in the pan. The sample was first heated in ultrapure nitrogen (20 mL/min) from room temperature to 300 °C at a heating rate of 10 °C/min to remove physisorbed species, then cooled to 50 °C and heated in air (20 mL/min) to 800 °C at a ramping rate of 10 °C/min.

2.4. Catalyst testing

The catalytic reaction was carried out in a fix-bed continuous flow glass reactor with an inside diameter of 12 mm under atmospheric pressure. The reactor was placed vertically inside a tubular furnace and heated electrically. The reactor temperature was monitored by a thermocouple with its tip located at the catalyst bed and connected to a temperature controller. The solution of reactants (molar ratio of aniline/glycerol = 3:1) was pumped through the preheater where it was vaporized and the reactants were carried into the reactor by flowing H₂ (20 mL/min), steam (6 mL/min) and N₂ (54 mL/min). The reaction was carried out at 220 °C. The total space velocity (SV) of raw materials and liquid hourly space velocity (LHSV) of reactants were 1700 h⁻¹ and 0.4 h⁻¹, respectively.

2.5. Product analysis

The products were analyzed on a gas chromatograph with a mass spectrometer (Agilent GC-MS 6890N-5975B) equipped with a HP-5 capillary column (0.25 mm, 30 m). The process was carried out in ultrapure helium gas from 90 °C to 230 °C at a heating rate of 5 °C/min and kept at the temperature for 30 min.

The quantitative analyses of the reactants and products were carried out on a SP-6890A gas chromatograph equipped with a SE-54 capillary column (0.32 mm, 30 m). 1-Hexyl alcohol was used as

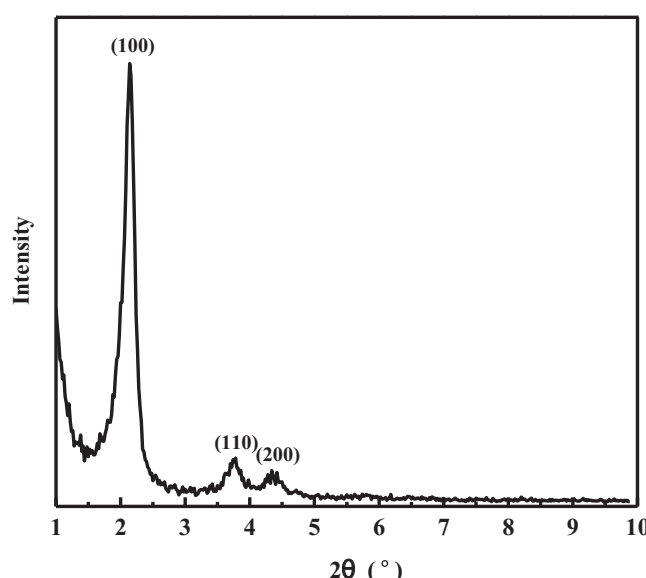


Fig. 1. XRD pattern of MCM-41 sample.

Table 1

The activity and selectivity of the copper catalysts supported on different zeolites.

Catalyst	Glycerol conversion (%)	Product selectivity (%)					
		3-MI	N-MA	N-EA	2,5-DMPP	2,3-DMI	Others
Cu/NaY	72.0	56.1	3.1	5.5	19.1	–	16.2
Cu/5A	65.3	32.2	1.4	44.2	6.8	–	15.4
Cu/HZSM-5	60.1	30.0	–	46.5	6.9	–	16.6
Cu/MCM-41	53.6	24.3	2.8	15.8	12.2	12.6	32.3

Reaction conditions: 220 °C, aniline/glycerol = 3:1 molar ratio, SV = 1700 h⁻¹, LHSV = 0.4 h⁻¹, H₂ = 20 mL/min, steam = 6 mL/min, N₂ = 54 mL/min. Copper loading: 5.4 wt%. The results were taken at the second hour.

an internal standard. The temperature programmed process was the same as GC-MS analysis with ultrapure nitrogen as the carrier gas.

The conversion of glycerol, the yield and selectivity of the product were calculated based on the following formulas:

$$\text{Conversion of glycerol}(\%) = \frac{\text{moles of glycerol converted}}{\text{moles of initial glycerol}} \times 100\%$$

with moles of glycerol converted = moles of initial glycerol – moles of final glycerol.

$$\text{Yield of product}(\%) = \frac{\text{moles of product formed}}{\text{moles of initial glycerol}} \times 100\%$$

$$\text{Selectivity of product}(\%) = \frac{\text{yield of product}}{\text{conversion of glycerol}} \times 100\%$$

3. Results and discussion

3.1. The synthesis of 3-methylindole over different zeolites supported copper catalysts

3.1.1. The activity and selectivity of different zeolites supported copper catalysts

In the reaction of glycerol and aniline over zeolite (NaY, 5A, HZSM-5 or MCM-41)-supported copper catalyst, except the aim product of 3-methylindole (3-MI), many by-products were produced. Among them, N-methylaniline (N-MA), N-ethylaniline (N-EA), 2,5-dimethyl-1-phenyl-pyrrole (2,5-DMPP) and 2,3-dimethylindole (2,3-DMI) were the major by-products, in addition, minor amounts of the other by-products were also detected, such as ethylic acid, N-isopropylaniline, N-propylaniline, propylene glycol, indole, 3-ketoneindole, N-isopropylindole and N,N'-dimethyl-N,N'-diphenyl-1,2-ethanediamine. The reaction pathway of glycerol and aniline to form the by-products is given in Scheme 2 [3,29,36–39].

Table 1 is the activity and selectivity of the copper catalyst supported on NaY, 5A, HZSM-5 or MCM-41. It can be seen that Cu/NaY exhibited higher activity and selectivity, which 72.0% glycerol conversion with 56.1% selectivity of 3-methylindole was obtained. Over Cu/5A or Cu/HZSM-5, N-ethylaniline was the major product and the selectivity of 3-methylindole was only 32.2 or 30.0%. Over Cu/MCM-41, larger amounts of undesired by-products were produced, which the selectivity of 3-methylindole was less than 25%.

3.1.2. Catalyst characterization

The specific surface area and pore volume on zeolite (NaY, 5A, HZSM-5 or MCM-41)-supported copper catalyst are presented in Table 2. It is clearly seen that Cu/MCM-41 possessed the largest specific surface area (801 m²/g) and pore volume (0.820 cm³/g), Cu/5A displayed the lowest specific surface area (453 m²/g) and Cu/HZSM-5 showed the lowest pore volume (0.156 cm³/g). Considering the activity and selectivity of the copper catalyst supported on NaY,

Table 2

Specific surface area and pore volume of the copper catalysts supported on different zeolites.

Catalyst	Specific surface Area (m ² /g)	Pore volume (cm ³ /g)
Cu/NaY	527	0.423
Cu/5A	453	0.250
Cu/HZSM-5	580	0.156
Cu/MCM-41	801	0.820

5A, HZSM-5 or MCM-41 zeolite, it can be obtained that the specific surface area or pore volume was not the crucial factor for the vapor-phase synthesis of 3-methylindole.

It is known that metal copper is the active component for the vapor-phase synthesis of 3-methylindole from glycerol and aniline who plays a crucial role in the production of 3-methylindole [30]. The better the copper particles was dispersed, the higher the activity was. Fig. 2 illustrates the XRD patterns of zeolites (NaY, 5A, HZSM-5 and MCM-41)-supported copper catalysts. Two small diffraction peaks of copper at 2θ of 43.3° and 50.5°, assigned to the (1 1 1) and (2 0 0) reflections, were observed on Cu/NaY [40]. On 5A, HZSM-5 or MCM-41-supported copper catalyst, the intensity of copper diffraction peaks was much stronger than that on Cu/NaY, meanwhile, another diffraction peak at 74.7°, assigned to the (2 2 0) reflection of copper, was observed and the intensity of copper diffraction peaks increased in the order of Cu/5A, Cu/HZSM-5 and Cu/MCM-41.

Based on the half peak width of (1 1 1) copper crystal phase, the average sizes of copper particles on Cu/NaY, Cu/5A, Cu/HZSM-5 and Cu/MCM-41 were calculated using the Scherrer Equation and the results were 18, 33, 39 and 49 nm, respectively. The average size of

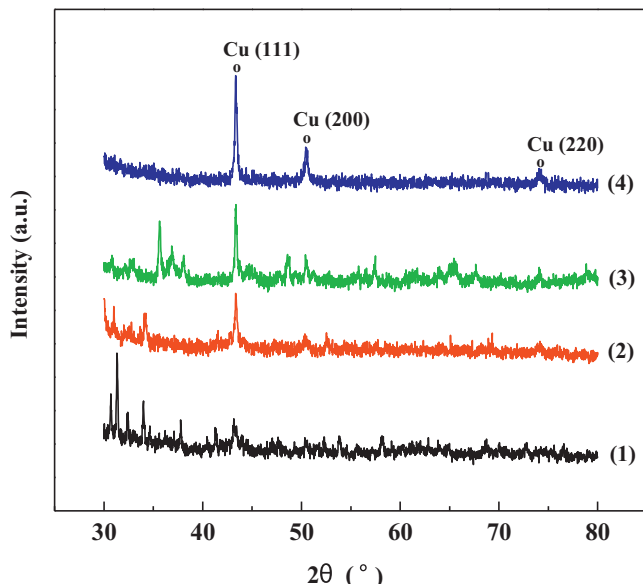
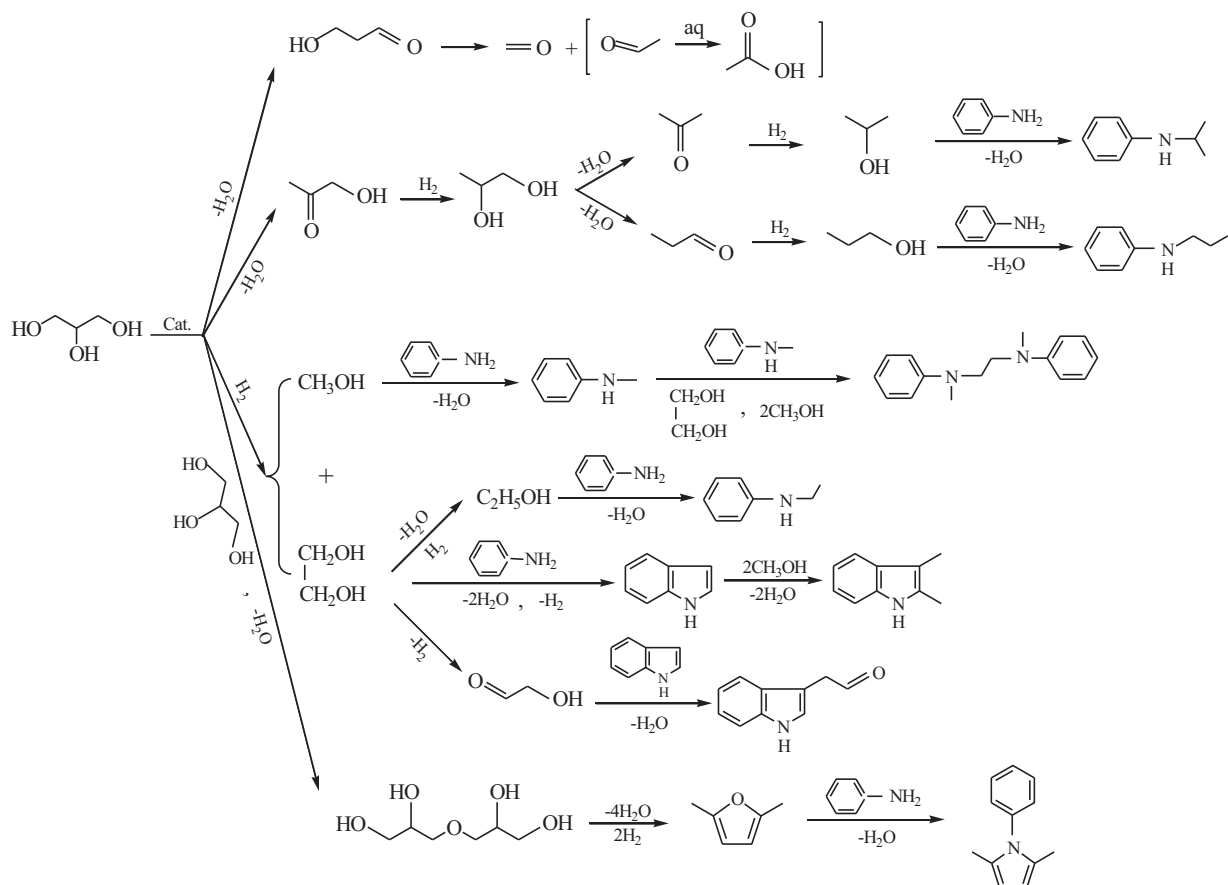


Fig. 2. XRD patterns of Cu/NaY (1), Cu/5A (2), Cu/HZSM-5 (3) and Cu/MCM-41 (4).



Scheme 2. The reaction pathway of glycerol and aniline to form the by-products over zeolite-supported copper catalyst.

copper particles on Cu/NaY was smallest compared with the other catalysts, suggested a better dispersion of the copper particles on the catalyst, while, on Cu/MCM-41, the average size of copper particles was the biggest although the catalyst possessed the largest specific surface area. This should be the reason that the interaction between copper particles and MCM-41 support was weak, which made the copper particles gather together easily, as a result, big copper particles could be formed on MCM-41 [41]. The interaction between copper and NaY, however, was relatively strong, which brought about the copper particles dispersed well on the support. From Fig. 2, Tables 2 and 3 it can be obtained that there was no correlation between the dispersion of copper particles and the specific surface area or pore volume. Taking the results of Tables 1 and 3 into account, it can be concluded that Cu/NaY with smaller copper particles was favorable to the synthesis of 3-methylindole.

Fig. 3 shows the acidity and acid strength distribution of zeolites-supported copper catalysts. More than two desorption peaks can be seen on the catalysts. The peaks at the lower temperature (<200 °C) were assigned to the weak acid sites, while the others at the higher temperature (200–400 °C) were corresponded to the middle-strong acid sites [42]. The areas of the weak acid sites on the zeolites-supported copper catalysts were observed to

decrease in the order of Cu/NaY, Cu/5A, Cu/HZSM-5 and Cu/MCM-41, while, the areas of the middle-strong acid sites decreased in the following sequence of Cu/NaY, Cu/MCM-41, Cu/5A and Cu/HZSM-5. Taking into account the results of NH₃-TPD and Table 1 it can be found that the more the weak acid sites, the higher the selectivity of 3-methylindole. Moreover, it seemed to be conduc-

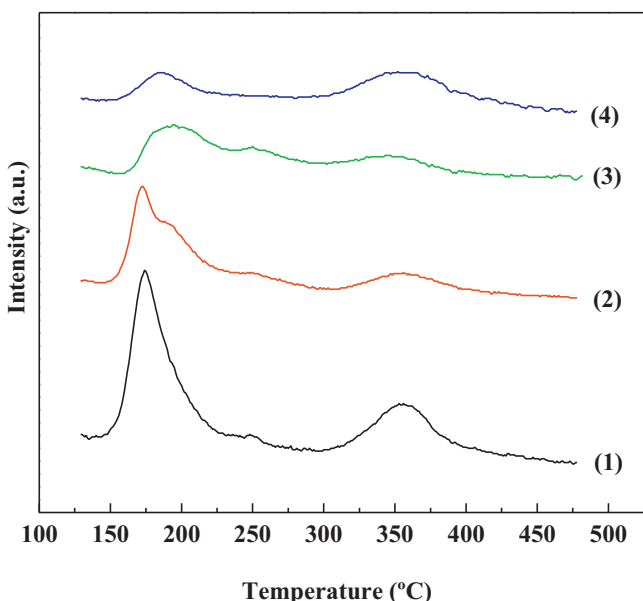


Fig. 3. NH₃-TPD profiles of Cu/NaY (1), Cu/5A (2), Cu/HZSM-5 (3) and Cu/MCM-41 (4).

Table 3

Average copper particle size of the copper catalysts supported on different zeolites.

Catalyst	Average copper particle size (nm)
Cu/NaY	18
Cu/5A	33
Cu/HZSM-5	39
Cu/MCM-41	49

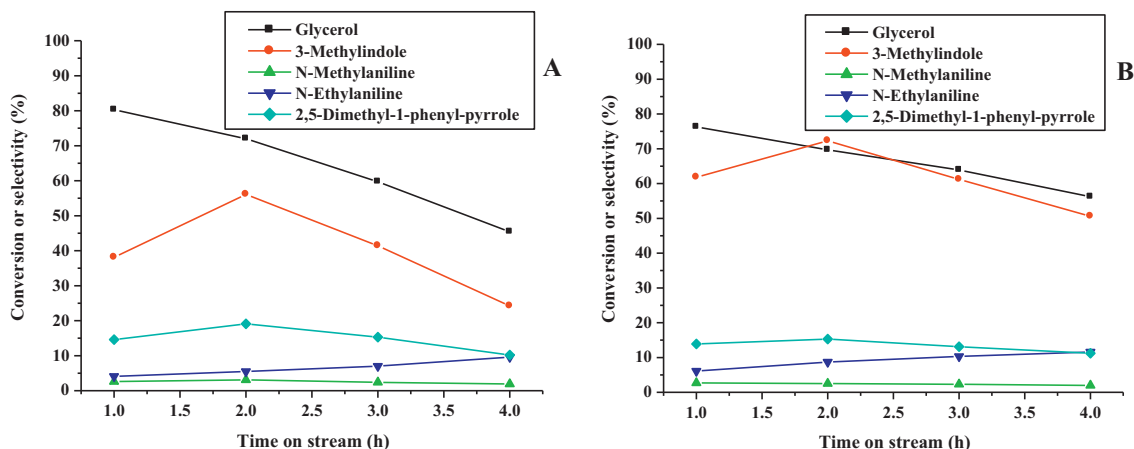


Fig. 4. Glycerol conversion and the selectivity to different products versus time on stream over Cu/NaY (A) or Cu/NaY-Na₂O (B).

tive to the formation of N-ethylaniline when the amount of the middle-strong acid sites was very small.

For the vapor-phase synthesis of 3-methylindole from glycerol and aniline, it is known that weak acid sites on Cu-based catalysts are favorable to the production of 3-methylindole because they can facilitate the adsorption of reactants on the surface of the catalyst. Middle-strong acid sites, however, take disadvantage of the reaction. Because 3-methylindole possesses weak alkalinity, it is difficult for 3-methylindole to desorb from the middle-strong acid sites, as a result, the further reaction could easily happen and bring about the decrease of 3-methylindole selectivity [30]. There were larger number of the weak acid sites and better dispersion of copper particles on Cu/NaY, therefore the catalyst exhibited higher activity and selectivity than Cu/5A, Cu/HZSM-5 or Cu/MCM-41.

3.2. The effect of Na₂O promoter on the performance of the Cu/NaY catalyst

From Fig. 3 it is known that there were many middle-strong acid sites on Cu/NaY, which can bring about some side reactions caused by 3-methylindole. In order to decrease the middle-strong acid sites on Cu/NaY, Na₂O was introduced into Cu/NaY and Table 4 exhibits the effect of Na₂O amount on the activity and selectivity of Cu/NaY-Na₂O catalyst. As expected, the selectivity of 3-methylindole increased remarkably after adding Na₂O to Cu/NaY although the conversion of glycerol decreased slightly. And with the increase of Na₂O amount, the selectivity of 3-methylindole increased first, then, decreased. When the amount of Na₂O was 0.60 mmol/g, the selectivity of 3-methylindole reached 72.3%, which the yield of 3-methylindole was up to 50.4%. From Fig. 3 it can also be found that the selectivity of N-ethylaniline increased

somewhat with the increase of Na₂O amount, while, the selectivity of N-methylaniline or 2,5-dimethyl-1-phenyl-pyrrole decreased.

Fig. 4 shows the activity and selectivity of Cu/NaY or Cu/NaY-Na₂O as a function of reaction time with Na₂O amount of 0.6 mmol/g. Over Cu/NaY, glycerol conversion decreased with time on stream rapidly, while, the selectivity of 3-methylindole increased during the first 2 h, then dropped. The changing trend to the selectivity of 2,5-dimethyl-1-phenyl-pyrrole was the same as 3-methylindole. The selectivity of N-methylaniline increased a little with time on stream, while, the selectivity of N-ethylaniline decreased slightly. A similar phenomenon was seen over Cu/NaY-Na₂O, but the selectivity of 3-methylindole were much higher than that over Cu/NaY and the decline greatly slowed down within the same period, indicating that Na₂O promoter had a substantial improvement not only in increasing the selectivity of 3-methylindole but also in decelerating the deactivation of the catalyst.

Fig. 5 shows the XRD patterns of NaY, the fresh or the used samples of Cu/NaY and Cu/NaY-Na₂O. Compared with the XRD pattern of the bare NaY support, no obvious change for the crystal diffraction peaks of NaY was observed on the fresh or the used Cu/NaY and Cu/NaY-Na₂O, suggested that the crystal structure of NaY was

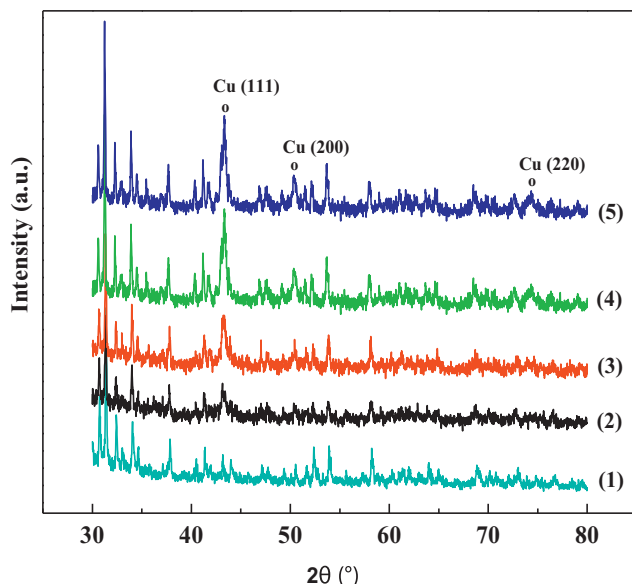


Fig. 5. XRD patterns of the fresh samples of NaY (1), Cu/NaY (2), Cu/NaY-Na₂O (3) and the used samples of Cu/NaY (4) and Cu/NaY-Na₂O (5).

Table 4
Effect of Na₂O amount on the activity and selectivity of Cu/NaY-Na₂O catalyst.

Na ₂ O Amount (mmol/g)	Glycerol conversion (%)	Product selectivity (%)				
		3-MI	N-MA	N-EA	2,5-DMPP	Others
0.0	72.0	56.1	3.1	5.5	19.1	16.2
0.2	71.1	60.3	2.9	6.3	17.6	12.9
0.4	70.5	65.5	2.7	7.6	16.0	8.2
0.6	69.7	72.3	2.5	8.7	15.3	1.2
0.8	68.9	65.2	2.2	9.8	13.5	9.3
1.0	67.8	60.5	2.0	10.9	11.4	13.2

Reaction conditions: 220 °C, aniline/glycerol = 3:1 molar ratio, SV = 1700 h⁻¹, LHSV = 0.4 h⁻¹, H₂ = 20 mL/min, steam = 6 mL/min, N₂ = 54 mL/min. Copper loading: 5.4 wt%. The results were taken at the second hour.

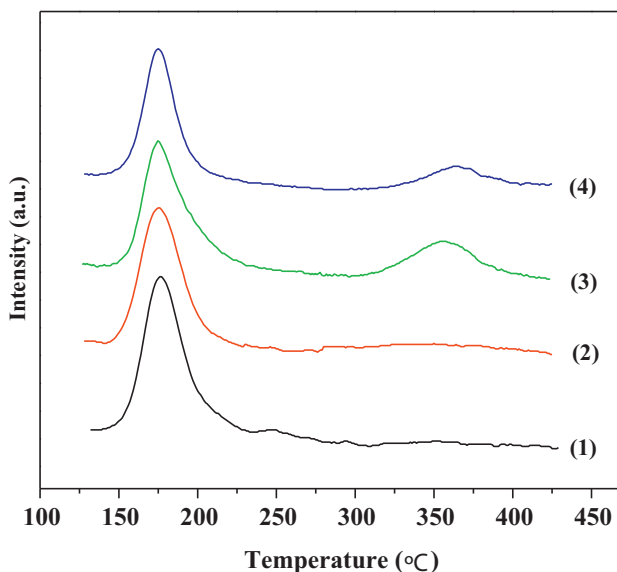


Fig. 6. NH₃-TPD profiles of NaY (1), NaY-Na₂O (2), Cu/NaY (3) and Cu/NaY-Na₂O (4).

remained well on the catalysts. On the fresh Cu/NaY, only two copper diffraction peaks can be seen, while, on the fresh Cu/NaY-Na₂O, three copper diffraction peaks were observed and the intensity was stronger than that on the fresh Cu/NaY catalyst. On the used NaY-supported copper catalysts, the intensity of copper diffraction peaks was much stronger than that on the fresh catalysts and the intensity of copper diffraction peaks was almost the same strong.

Table 5 presents the average sizes of copper particles on the fresh or the used Cu/NaY and Cu/NaY-Na₂O based on the Scherrer Equation. It can be seen that the average size of copper particles on the fresh Cu/NaY-Na₂O was bigger than that on the fresh Cu/NaY, indicated that the addition of Na₂O to Cu/NaY did not promote the dispersion of copper particles on the support. Compared with the fresh catalysts, the average sizes of copper particles on the used Cu-based catalysts became much bigger, suggested that there existed the sintering of copper particles during the reaction. On the used Cu/NaY-Na₂O, the average size of copper particles was the same as that on the used Cu/NaY, revealed that Na₂O did not aggravate the sintering of copper particles.

Fig. 6 shows the NH₃-TPD profiles of NaY, NaY-Na₂O, Cu/NaY and Cu/NaY-Na₂O. On NaY or NaY-Na₂O, there existed a lot of weak acid sites, while, few or no middle-strong acid sites was observed. On NaY supported copper catalyst, the amount of the weak acid sites decreased slightly, however, large amount of the middle-strong acid sites appeared at about 360 °C. After adding Na₂O to Cu/NaY, the amount of the weak acid sites or the middle-strong acid sites decreased and the amount of the middle-strong acid sites decreased more remarkably.

From the experiments it was known that NaY or NaY-Na₂O exhibited very low activity and selectivity with the yield of 3-methylindole less than 8%, which revealed again that metal copper is the active component for the vapor-phase synthesis of 3-methylindole from glycerol and aniline [30]. Because Na₂O

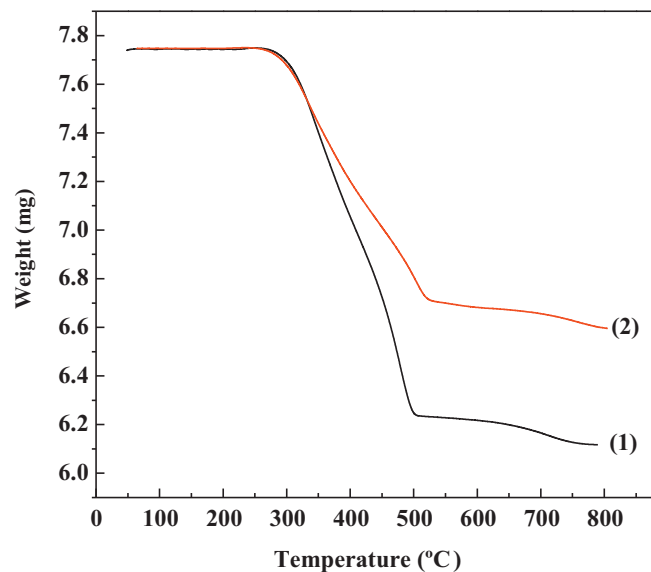


Fig. 7. TG curves of the used samples of Cu/NaY (1) and Cu/NaY-Na₂O (2).

decreased the amount of the middle-strong acid sites clearly, the selectivity of 3-methylindole increased greatly.

TG-DTA analysis was used to investigate the coke formation of the used Cu/NaY and the catalyst modified by Na₂O. The results are shown in Figs. 7 and 8. From Fig. 7 the obvious mass loss was observed on the catalysts, indicated that there existed the formation of coke during the reaction. On the used Cu/NaY-Na₂O, the mass loss was much less than that on the used Cu/NaY, revealed that Na₂O could inhibit the formation of the coke effectively. From Figs. 6 and 7, it can easily be found that the amount of the coke was relevant to the amount of acid sites on the catalyst. With fewer acid sites, there was less coke.

In Fig. 8, two exothermic peaks were observed, indicated that there existed two types of coke. The exothermic peak at 340 °C was assigned to the removal of easily oxidized carbon, while, another exothermic peak at 484 °C was the oxidation of regular or graphitic carbon [43]. After adding Na₂O to Cu/NaY, the amount of the easily oxidized carbon increased, while, the amount of regular or graphitic

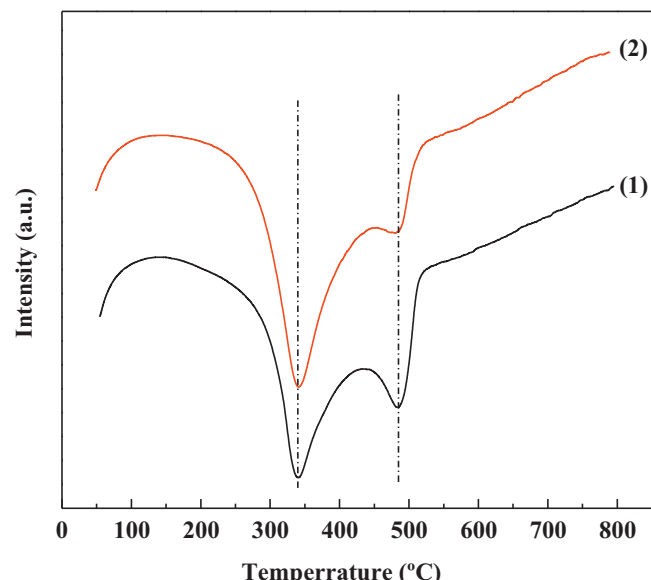
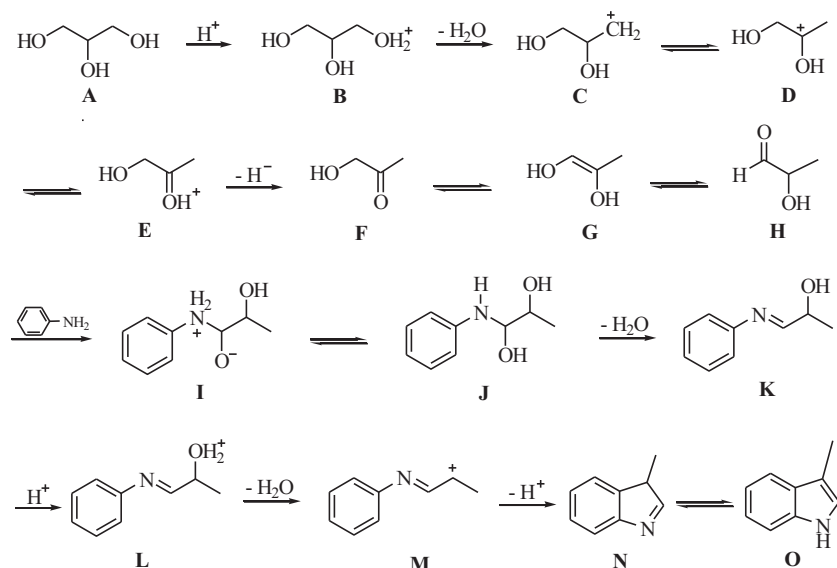


Fig. 8. DTA profiles of the used samples of Cu/NaY (1) and Cu/NaY-Na₂O (2).

Table 5
Average copper particle size of Cu/NaY and Cu/NaY-Na₂O.

Catalyst	Average copper particle size (nm)	
	Fresh sample	Used sample
Cu/NaY	18	41
Cu/NaY-Na ₂ O	23	41



Scheme 3. A probable mechanism for the synthesis of 3-methylindole from glycerol and aniline over zeolites-supported Cu-based catalysts.

carbon decreased. Compared with the used Cu/NaY, there was no obvious shift for the temperature of the exothermic peaks on the used Cu/NaY-Na₂O, indicated that the texture of the coke was not changed after adding Na₂O to Cu/NaY.

3.3. Probable catalytic mechanism for the vapor-phase synthesis of 3-methylindole

It has been reported that glycerol can adsorb on acid sites and be converted to different products through the intermediate of acetol [7,44–46]. In order to shed light on the catalytic synthesis mechanism of 3-methylindole from glycerol and aniline over zeolites-supported Cu-based catalysts, the reaction products of glycerol with aniline were carefully analyzed by GC-MS. In addition, the conversion of glycerol over the catalysts was also investigated and acetol was found as the major product. Taking into account the experimental results and the relevant literatures [46–50], a probable mechanism for the catalytic synthesis of 3-methylindole was hypothesized (Scheme 3).

Glycerol was firstly treated by protonation and dehydration to form the carbocation (C). C, then, underwent rearrangement to give the intermediate of D or E. E was subsequently converted to acetol (F) by losing a hydrogen proton [7,45–47], and F was readily transformed to 2-hydroxy-1-propanal (H) via enol-keto tautomerism. The amine cation (I) was formed through the reaction of H with aniline, and I underwent the migration of hydrogen proton and dehydrated to form the imine (K) [46,47]. A hydrogen proton was soon transferred to K to form the intermediate (L), and L was finally converted to the aim product of 3-methylindole by dehydration and eliminating a hydrogen proton.

It should be noted especially that copper particles with high dispersion played an important role in the synthesis of 3-methylindole from glycerol and aniline because their empty orbitals could receive the electrons from glycerol or aniline, which was favorable for the adsorption of reactants on the surface of catalyst. More importantly, Cu had a good catalytic activity to the cleavage of C–O bond [47,51] which promoted the formation of C, K or M. In the reaction, therefore, copper particles and weak acid sites acted together to promote the synthesis of 3-methylindole.

4. Conclusions

The vapor-phase synthesis of 3-methylindole from glycerol and aniline over zeolites-supported copper-based catalysts was studied. Cu/NaY catalyst, in terms of both the conversion of glycerol and the selectivity to 3-methylindole, was found to be better than 5A, HZSM-5 or MCM-41-supported copper catalyst, which the yield of 3-methylindole reached 40.3%. The higher activity and selectivity of Cu/NaY stemmed from its better dispersion of copper particles and larger amount of the weak acid sites. The addition of Na₂O to Cu/NaY not only increased the selectivity of the catalyst remarkably, which 72.3% selectivity with 50.4% yield for 3-methylindole was achieved, but also decelerated the deactivation of the catalyst, because Na₂O could decrease the amount of middle-strong acid sites of the catalyst remarkably and inhibit the formation of the coke during the reaction. Adding Na₂O to Cu/NaY did not change the texture of the coke. Based on the results of the experiments and the relevant literatures, a possible mechanism for the synthesis of 3-methylindole from glycerol and aniline over zeolites-supported Cu-based catalysts was proposed, in which acetol was the intermediate to produce 3-methylindole.

Acknowledgement

We gratefully acknowledge the financial support provided by the National Natural Science Foundation of China (No. 21173110).

References

- [1] T. Miyazawa, Y. Kusunoki, K. Kunimori, K. Tomishige, *J. Catal.* 240 (2006) 213–221.
- [2] A. Behr, J. Eilting, K. Irawadi, J. Leschinski, F. Lindner, *Green Chem.* 10 (2008) 13–30.
- [3] I. Gandarias, P.L. Arias, J. Requies, M.B. Güemez, J.L.G. Fierro, *Appl. Catal. B* 97 (2010) 248–256.
- [4] W. Suprun, M. Lutecki, T. Haber, H. Papp, *J. Mol. Catal. A* 309 (2009) 71–78.
- [5] J. George, Y. Patel, S.M. Pillai, P. Munshi, *J. Mol. Catal. A* 304 (2009) 1–7.
- [6] R.B. Mane, C.V. Rode, *Green Chem.* 14 (2012) 2780–2789.
- [7] F. Cavanì, S. Guidetti, L. Marinelli, M. Piccinini, E. Ghedini, M. Signoretto, *Appl. Catal. B* 100 (2010) 197–204.
- [8] D. Liang, J. Gao, H. Sun, P. Chen, Z.Y. Hou, X.M. Zheng, *Appl. Catal. B* 106 (2011) 423–432.

- [9] R.K.P. Purushothaman, J. Haveren, D.S. Es, I. Melián-Cabrera, H.J. Heeres, *Green Chem.* 14 (2012) 2031–2037.
- [10] L. Li, T.I. Korányi, B.F. Sels, P.P. Pescarmona, *Green Chem.* 14 (2012) 1611–1619.
- [11] L.J. Zhu, P.J. Guo, X.W. Chu, S.R. Yan, M.H. Qiao, K.N. Fan, X.X. Zhang, B.N. Zong, *Green Chem.* 10 (2008) 1323–1330.
- [12] S. Kamijo, Y. Yamamoto, *J. Org. Chem.* 68 (2003) 4764–4771.
- [13] D.G. Hulcoop, M. Lautens, *Org. Lett.* 9 (2007) 1761–1764.
- [14] C.S. Xie, Y.H. Zhang, Z.D. Huang, P.Z. Xu, *J. Org. Chem.* 72 (2007) 5431–5434.
- [15] M. Howe-Grant, Kirk-Othmer Encyclopedia of Chemical Technology, 4th ed., New York : John Wiley & Sons, 1995, p. 161.
- [16] M. Howe-Grant, Kirk-Othmer Encyclopedia of Chemical Technology, 3rd ed., New York : John Wiley & Sons, 1989, p. 213.
- [17] E. Doran, F.W. Whittington, J.D. Wood, J.D. McGivan, *Chem. Biol. Interact.* 140 (2002) 81–92.
- [18] G. Chen, R.A. Cue, K. Lundstrom, J.D. Wood, O. Doran, *Drug Metab. Dispos.* 36 (2008) 56–60.
- [19] J.M. Weems, G.S. Yost, *Chem. Res. Toxicol.* 23 (2010) 696–704.
- [20] B. Deslandes, C. Gariépy, A. Houde, *Livest. Prod. Sci.* 71 (2001) 193–200.
- [21] M. Bandini, A. Eichholzer, *Angew. Chem. Int. Ed.* 48 (2009) 9608–9644.
- [22] G.R. Humphrey, J.T. Kuethe, *Chem. Rev.* 106 (2006) 2875–2911.
- [23] C.A. Simoneau, A.M. Strohl, B. Ganem, *Tetrahedron Lett.* 48 (2007) 1809–1811.
- [24] M.A. Fox, D.A. Chandler, C. Lee, *J. Org. Chem.* 56 (1991) 3246–3255.
- [25] B. Robinson, *Chem. Rev.* 63 (1963) 373–401.
- [26] P. Magnus, L.S. Mitchell, *Tetrahedron Lett.* 39 (1998) 4595–4598.
- [27] C.S. Cho, J.H. Kim, T.J. Kim, S.C. Shim, *Tetrahedron* 57 (2001) 3321–3329.
- [28] D.V. Gopal, B. Srinivas, V. Durgakumari, M. Subrahmanyam, *Appl. Catal. A* 224 (2002) 121–128.
- [29] M. Campanati, S. Franceschini, O. Piccolo, A. Vaccari, *J. Catal.* 232 (2005) 1–9.
- [30] W. Sun, D.Y. Liu, H.Y. Zhu, L. Shi, Q. Sun, *Catal. Commun.* 12 (2010) 147–150.
- [31] M. Karthik, C.J. Magesh, P.T. Preumal, M. Palanichamy, B. Arabindoo, V. Murugesan, *Appl. Catal. A* 286 (2005) 137–141.
- [32] M.A. Alotaibi, E.F. Kozhevnikova, I.V. Kozhevnikov, *J. Catal.* 293 (2012) 141–144.
- [33] J.K. Nam, M.J. Choi, D.H. Cho, J.K. Suh, S.B. Kim, *J. Mol. Catal. A* 370 (2013) 7–13.
- [34] T. Subramanian, M. Kumaraja, K. Pitchumani, *J. Mol. Catal. A* 363–364 (2012) 115–121.
- [35] L.Y. Chen, T. Horiuchi, T. Mori, K. Maeda, *J. Phys. Chem. B* 103 (1999) 1216–1222.
- [36] M.Á. Aramendia, V. Borau, C. Jiménez, J.M. Marinas, F.J. Romero, *Appl. Catal. A* 183 (1999) 73–80.
- [37] S. Narayanan, A. Sultana, *Appl. Catal. A* 167 (1998) 103–111.
- [38] J. Liu, C.M. Li, X.M. Huo, L. Shi, Q. Sun, *Chin. J. Catal.* 29 (2008) 159–162.
- [39] L.C.A. Oliveira, M.F. Portilho, A.C. Silva, H.A. Taroco, P.P. Souza, *Appl. Catal. B* 117–118 (2012) 29–35.
- [40] D.H. Ji, W.C. Zhu, Z.L. Wang, G.J. Wang, *Catal. Commun.* 8 (2007) 1891–1895.
- [41] Y.J. Huang, H.P. Wang, J.F. Lee, *Chemosphere* 50 (2003) 1035–1041.
- [42] D.F. Jin, Z.Y. Hou, L.W. Zhang, X.M. Zheng, *Catal. Today* 131 (2008) 378–384.
- [43] N.A. Hermes, M.A. Lansarin, O.W. Perez-Lopez, *Catal. Lett.* 141 (2011) 1018–1025.
- [44] Y. Kusunoki, T. Miyazawa, K. Kunimori, K. Tomishige, *Catal. Commun.* 6 (2005) 645–649.
- [45] Z.L. Yuan, L.N. Wang, J.H. Wang, S.X. Xia, P. Chen, Z.Y. Hou, X.M. Zheng, *Appl. Catal. B* 101 (2011) 431–440.
- [46] S.H. Zhu, Y.L. Zhu, S.L. Hao, H.Y. Zheng, T. Mo, Y.W. Li, *Green Chem.* 14 (2012) 2607–2616.
- [47] M.A. Dasari, P.P. Kiatsimkul, W.R. Sutterlin, G.J. Suppes, *Appl. Catal. A* 281 (2005) 225–231.
- [48] M. Campanati, A. Vaccari, O. Piccolo, *Catal. Today* 60 (2000) 289–295.
- [49] A. Corma, G.W. Huber, L. Sauvauaud, P. O'Connor, *J. Catal.* 257 (2008) 163–171.
- [50] J.J. Li, Name Reactions A Collection of Detailed Reaction Mechanisms, 3rd ed., Springer, Berlin, Heidelberg, 2006, pp. 545.
- [51] Z.W. Huang, F. Cui, H.X. Kang, J. Chen, X.Z. Zhang, C.G. Xia, *Chem. Mater.* 20 (2008) 5090–5099.